

# **Study on stratospheric gravity wave activity: Global and seasonal variations deduced from the CHALLENGING Minisatellite Payload (CHAMP)-GPS Satellite**

**M. Venkat Ratnam and Christoph Jacobi**

## **Abstract**

Global analyses of gravity wave activity in the stratosphere are presented for the first time using German Low Earth Orbit (LEO) satellite CHAMP. Temperature profiles obtained from CHAMP/GPS radio occultations are first compared with ground based instruments. In general, good agreement is found between these different techniques. Monthly mean  $E_p$  values of potential energy,  $E_p$  values, being a measure of gravity wave activity, which is estimated with radiosonde observations are compared with CHAMP/GPS data and found that radiosonde observed  $E_p$  values are higher than those estimated with radio occultations. There exists a strong diurnal variation of gravity wave activity. From the global morphology of gravity wave activity, large values  $E_p$  are noticed even at mid latitudes during winter months besides the tropical latitudes but not during equinoxes suggesting that wave activity, especially at stratospheric heights, is not only modulated due to orography (mountain/lee waves) but mainly depends on seasonal variations at respective latitudes. Latitudinal and vertical variation of gravity wave activity reveals the existence of large  $E_p$  values below 25 km and low values in between 25 and 30 km in all the seasons near equator. During southern hemisphere winter, large values are noticed. During equinoxes, these values are nearly same between northern and southern hemispheres (NH and SH) at mid-latitudes. During the months of solstices,  $E_p$  distribution involves a larger hemispheric asymmetry at middle and higher latitudes. Large values of  $E_p$  are noticed at SH polar latitudes during Sep-Oct months and the latitude range is wider ( $\pm 30^\circ$  latitude in both the hemispheres) with large  $E_p$  values in all the seasons except winter.

## **Zusammenfassung**

Zum ersten Mal werden globale Analysen der Schwerewellenaktivität, bestimmt unter Verwendung des CHAMP LEO-Satelliten, vorgestellt. Temperaturprofile der CHAMP/RO-Okkultationen werden zunächst mit bodengestützten Messungen verglichen. Generell ist die Übereinstimmung gut. Monatliche Mittelwerte der potentiellen Energie  $E_p$ , die als Maß für Schwerewellenaktivität gilt, wurden aus Radisonden- und CHAMP-Messungen bestimmt, wobei die CHAMP-Daten höhere Werte lieferten. Es existiert eine deutlicher Tagesgang von  $E_p$ . Die globale Morphologie der Schwerewellenaktivität zeigt hohe Werte nicht nur am Äquator, sondern auch in mittleren Breiten, dies aber nicht während der Äquinoktien. Dies weist darauf hin, dass Schwerewelleaktivität nicht nur orographisch angetrieben ist, sondern in verschiedenen Breiten vom Jahresgang abhängt. Die Breiten- und Höhenabhängigkeit der Schwerewellenaktivität zeigt zwischen 25 und 30 km niedrige, unterhalb von 25 km hohe Werte von  $E_p$  am Äquator. Während des Winters in der Südhemisphäre sind die Werte hoch, während zu den Äquinoktien hohe Werte in mittleren Breiten beider Hemisphären zu finden sind. Während der Solstitien zeigt die  $E_p$ -Verteilung stärkere hemisphärische Asymmetrie. Hohe Werte von  $E_p$  werden während des südpolaren Frühjahrs gemessen. Der äquatoriale Bereich hoher Varianz ist in allen Jahreszeiten außer im Winter breit ( $\pm 30^\circ$ ).

## 1. Introduction

Gravity waves play a crucial role in driving the general circulation of the middle atmosphere. Inclusion of gravity waves effects, by employing various parameterisations, has become necessary for accurate general circulation modelling. These waves cause fluctuations in velocity, pressure and density in a sinusoidal nature. Moreover they carry momentum flux and energy with them as they propagate. Most of the sources for the generation of these gravity waves lie in the troposphere [Fritts and Nastrom, 1992]. In the tropics, it is generally thought that gravity waves are mostly generated by cumulus convection [Alexander and Holton, 1997; Piani et al., 2000; Alexander et al., 2000 and references therein]. Recently, Beres et al. [2002] stressed the importance of tropospheric wind shears and its essential include in any attempt to parameterise the effects of gravity wave activity. These waves will propagate upward with increasing amplitude and have ability to transfer momentum and energy, and deposit in upper atmosphere through dissipation. All the gravity waves generated in the lower troposphere will not propagate equally in all directions. Gravity waves with longer periods will propagate at large zenith angles and can reach upper atmosphere whereas short period waves propagate off-zenith with small zenith angles and dissipate their energy quickly [Kiffaber et al., 1993].

During the past two decades, considerable effort has been devoted in characterizing these gravity waves with the advent of VHF radars and lidars. Unfortunately these radars are blank in upper stratosphere, and lidars have served the best to fill this gap. Even though these techniques can provide observations with excellent time and spatial resolutions but the network of these ground based instruments is very small and hence global morphology of gravity wave activity is poorly know with these techniques. Satellite observations are able to provide global coverage [Wu and waters, 1996; McLandress et al., 2000] but are of poor spatial resolution and are not suitable to retain the spectral properties of gravity waves but can give quantitative picture of wave activity. Recently using GPS/MET satellite observations, Tsuda et al., [2000] provided the global analysis of stratospheric gravity wave activity with special emphasis during winter months. Using same data, Nastrom et al. [2000] had compared the gravity wave energy observed by the VHF radar with GPS/MET data. In the present study, global analysis of gravity wave activity observed by CHAMP/GPS satellite is presented with more statistical results. The data used in the present study is almost twice than seen by GPS/MET which was possible due to latest occultation antenna geometry that allowed the soundings with high accuracy and high vertical resolution. Few more interesting features has been noticed besides those reported by Tsuda et al., [2000] and possible reasons for the observed significant results has been presented in this study.

## 2. Brief system description and data base

The CHAMP/GPS satellite was launched on July 15, 2000 from Plesetsk (62.5<sup>0</sup>N, 40.3<sup>0</sup>E) using a Russian COSMOS rocket into an almost circular and near polar orbit (inclination 87<sup>0</sup>) with an initial altitude of 454 km. It consists of mainly seven parts: an electrostatic STAR accelerometer is used for measuring non-gravitational accelerations; a TRSR-2 GPS receiver serves as the main tool for high-precision orbit determination of the CHAMP/GPS satellite; a laser Retro Reflector is used to reflect short laser pulses back to the transmitting ground station enabling to measure the direct two way range between the ground station and satellite; a fluxgate magnetometer is the prime instrument for magnetic field investigations, while an Overhauser magnetometer provides an absolute in-flight calibrations capability. An Advanced Stellar Compass provides processing power for the image analysis, pattern recognition, data reduction, system protection and communication. A digital ion drift meter is used to make in-situ measurements of the ion distribution and its movement with in the ionosphere. This drift

meter is operated in combination with a Langmuir probe for in situ electron density measurements. More details of the system can be had from *Reigber et al.* [2000].

For the present study we use level-2 data, which are produced by GfZ Potsdam using standard methods for occultation processing. The atmospheric excess path is derived using a double diffraction technique and atmospheric profiles are calculated assuming a geometric optics approach and applying Abel inversion technique [*Hocke, 1997*]. The first occultation measurements from CHAMP/GPS was performed on February 11, 2001, since then for about 200-250 occultations were recorded daily. The data used for the present study starts from May 2001 through September 2002. Besides this data, temperature observed with ground based instruments (radiosonde and lidar) are also collected during the above mentioned periods to compare with CHAMP/GPS data. Throughout the observational period, anti-spoofing (A/S) was activated, but the data quality is regained unlike GPS/MET by using latest occultation antenna geometry, which allowed the soundings with high accuracy and vertical resolution [*Wickert et al., 2001*]. More details of the data analysis, its processing, initial results of the CHAMP/GPS and validation with the corresponding global weather analysis can be had from *Wickert et al.* [2001].

### 3. Methodology for calculation of gravity wave energy density

Atmospheric parameters fluctuate on a wide range of scales. In the mesoscale, wind and temperature fluctuations are sometimes described by using frequency ( $\omega$ ) and wave number ( $m$ ,  $k$ ) power spectra since they are observed as a superposition of many waves with various frequencies and wave numbers. The modelling of atmospheric gravity wave spectra has followed the pioneering efforts of *Garret and Munk* [1972; 1975], who developed a dynamical theory for the spectrum of internal waves in the ocean. The key element of the *Garret and Munk* model is that the waves obey the polarization and dispersion relations. Since then several gravity wave spectral models have been developed for comparison with MST Radar experiments [*VanZandt 1982, 1985; Scheffler and Liu, 1985, 1986; Fritts and VanZandt, 1987*].

Under linear gravity wave theory, neglecting the effects of the background wind, *Scheffler and Liu* [1985] derived an equation relating the observed one-dimensional frequency spectrum to the *Garret-Munk* model gravity wave spectrum [*Garret and Munk 1972*]. For Boussinesq approximation, the one dimensional frequency spectrum is defined as

$$E_{ob}(\omega) = E_0 H_0(\omega) B(\omega), \quad (1)$$

Where the filter function  $H_0(\omega)$  can be expressed as

$$H_0(\omega) = \frac{\omega^2 - \omega_i^2}{\omega_b^2 - \omega_i^2} \cos^2 \theta_B + \frac{1}{2} \frac{\omega_b^2 - \omega^2}{\omega_b^2 - \omega_i^2} \left( 1 + \frac{\omega_i^2}{\omega^2} \right) \sin^2 \theta_B, \quad (2)$$

and

$$B(\omega) = \frac{p-1}{\omega_i^{1-p} - \omega_b^{1-p}} \omega^{-p}. \quad (3)$$

$E_0$  is the energy density constant. Therefore

$$E_{ob}(\omega) = E_0 \frac{p-1}{\omega_i^{1-p} - \omega_b^{1-p}} \omega^{-p} \left( \frac{\omega^2 - \omega_i^2}{\omega_b^2 - \omega_i^2} \cos^2 \theta_B + \frac{1}{2} \frac{\omega_b^2 - \omega^2}{\omega_b^2 - \omega_i^2} \left( 1 + \frac{\omega_i^2}{\omega^2} \right) \sin^2 \theta_B \right), \quad (4)$$

where  $\theta_B$  is the direction of wave propagation and  $\omega_b$ ,  $\omega_i$  are the Brunt-Väisälä frequency and inertial frequency, respectively.  $P$  is the frequency power law index. While deriving Eq. (4) it

is also assumed that the wave frequency and wave number are separable in the *Garret-Munk* model spectrum.

The energy density  $E_0$  is chosen as a measure of gravity wave activity and is defined as [see, e.g., *Tsuda et al.*, 2000]

$$E_0 = \frac{1}{2} \left[ u'^2 + v'^2 + w'^2 + \left( \frac{g}{N} \right)^2 \left( \frac{T'}{T} \right)^2 \right] = E_k + E_p, \quad (5)$$

where  $E_k$  and  $E_p$  are kinetic and potential energy per unit mass, respectively. They can be written as

$$E_k = \frac{1}{2} [u'^2 + v'^2 + w'^2], \quad (6)$$

$$E_p = \frac{1}{2} \left( \frac{g}{N} \right)^2 \left( \frac{T'}{T} \right)^2, \quad (7)$$

where

$$N^2 = \frac{g}{T} \left( \frac{dT}{dz} - \Gamma \right). \quad (8)$$

Here  $u'$ ,  $v'$  and  $w'$  are the perturbation components of the zonal, meridional and vertical wind respectively,  $g$  is the acceleration due to gravity,  $N$  is the Brunt-Väisälä frequency,  $T$  and  $T'$  are the mean and perturbation components of temperature and  $\Gamma$  is the dry adiabatic lapse rate. According to the linear theory of the gravity waves, the ratio of kinetic to potential energy becomes constant, therefore it is possible to estimate  $E_0$  from temperature observations only [*Tsuda et al.*, 2000]. In Eq. (7), the calculation of  $E_p$  mainly depends on the estimation of the temperature fluctuation. For this, the procedure adopted by *Tsuda et al.*, [2000], i.e., calculating temperature fluctuation by high-pass filter with a cut-off at 10 km is closely followed here.

## 4. Results and discussion

### 4.1. Comparison of CHAMP data with ground based instruments

Before going into details of the gravity wave activity seen by the CHAMP/GPS satellite, it is desirable to compare the observed temperature profiles with some reference techniques. The first observations have been compared with corresponding ECMWF profiles in the height range of 5 and 25 km and found excellent comparison within 1 K in both hemispheres, but some negative bias at tropical latitudes [*Wickert et al.*, 2001]. In the present study, temperature observed with radiosonde (10-30 km) over two stations, one at a tropical latitude (13.5°N, 79.2°E) and other at subtropical latitude (25°N, 121°E) and also with lidar (30 to 60 km) located at a tropical station has been selected to compare with CHAMP/GPS data. In order to reduce the error due to the temporal and spatial difference of the CHAMP data,  $\pm 2^\circ$  in latitude,  $\pm 60^\circ$  in longitude and  $\pm 2$  hours has been selected as best coincidence with that of ground based instruments. Figure 1 shows the comparison of vertical profiles of temperature between CHAMP, radiosonde and lidar observed on March 4, 2002 (left panel) and May 1, 2002 (right panel). From the figure it is clear that generally CHAMP and ground based observed profiles are matching well. There exists some difference below 5 km (sometimes up to 10 km) and above 40-45 km, which is due to water vapour and ionospheric residuals that occur from incomplete ionospheric correction in the temperature retrieval from the GPS occul-

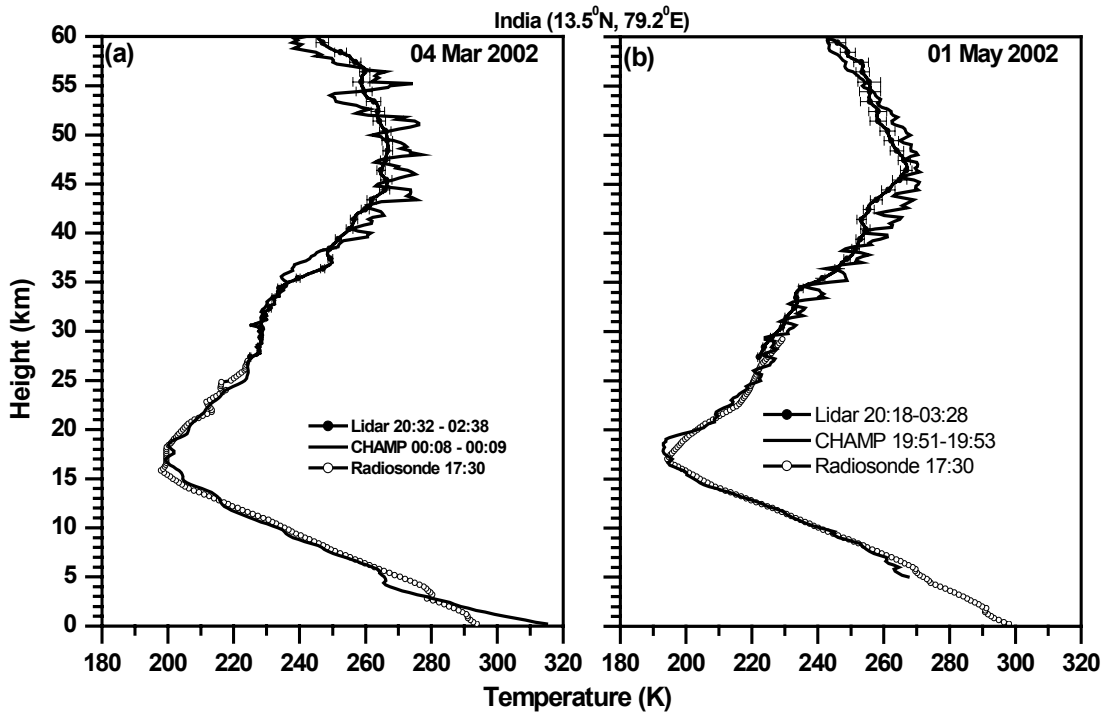


**Figure 1:** Vertical profiles of temperature observed by CHAMP/GPS, a radiosonde and a Lidar located at Gadanki ( $13.5^{\circ}\text{N}$ ,  $79.2^{\circ}\text{E}$ ) on (a) March 4, 2002 and (b) May 1, 2002.

tation method at these heights. Hence we will restrict our studies to the height range between 10 and 45 km only. In addition, one can see some bias in CHAMP data near the tropopause, sometimes showing high temperatures and sometimes low temperatures.

Extensive comparison between different techniques is shown in Figure 2. This figure shows scatter plots of temperatures observed by CHAMP vs. radiosonde (left panel) in between 10 and 30 km and CHAMP vs. lidar (right panel) between 30 and 60 km during May 2001 to June 2002. From the figure it can be seen that between 10 and 30 km for about 95% of the time the temperature is matching well (from 213 profiles of near coincidence) and the error is only larger near the tropopause. Above 30 km, for about 90% of the time the temperature is matching well (from 31 profiles) and larger errors are only found above the 45 km height region, a result that is expected due to ionospheric residuals. In general, the overall comparison of CHAMP data with ground based instruments is matching well.

#### 4.2. Gravity wave potential energy observed with CHAMP/GPS and radiosonde

In this section, estimations of  $E_p$  from the temperature perturbations,  $T'$ , using ground based instruments and CHAMP data are presented. Figure 3a shows the vertical profiles of temperature observed with CHAMP/GPS (0.2 to 60 km), radiosonde (0 to 27 km), and lidar (27 to 60 km) observed on March 4, 2002. In order to see the temperature fluctuation defined as deviations from the mean, monthly averaged profiles of temperature observed with radiosonde and lidar are also plotted in the same figure. The overall comparison between these various techniques show that the variations generally are matching well. Figure 3b shows  $T'$  that here is observed when instant observations are subtracted from monthly mean. From this figure it is clear that there exist large fluctuations and the estimation of potential energy using these perturbations will lead to unrealistic values. Instead of this,  $T'$  is estimated from the

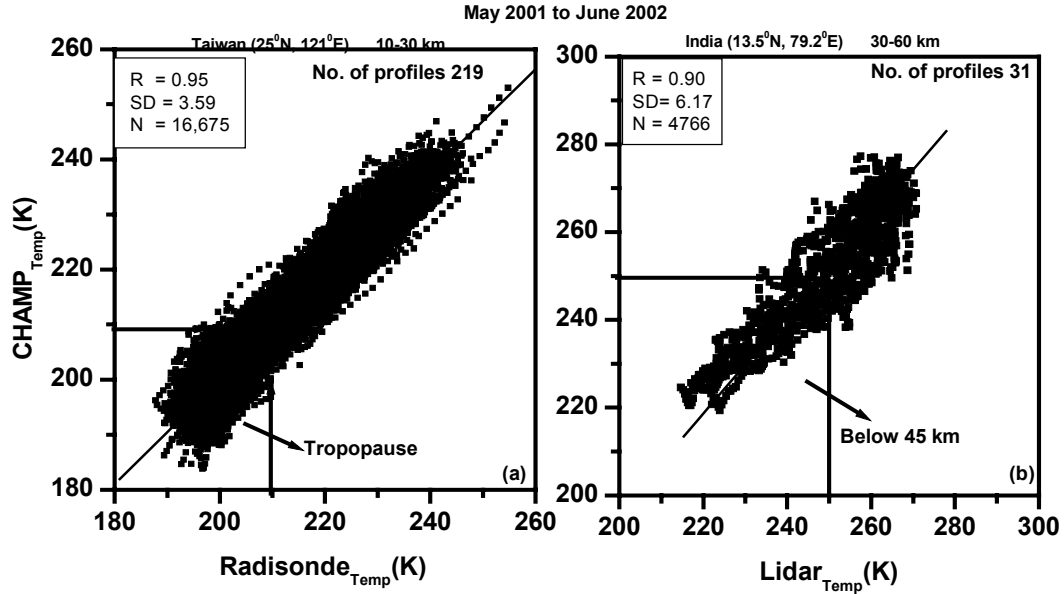


**Figure 2:** Comparison of temperature observed between (a) CHAMP and radiosonde (10-30 km) and (b) CHAMP and lidar (30-60 km) during May 2001 to June 2002.

single CHAMP profile by applying a high pass filter with a cut-off at 10 km as followed by *Tsuda et al.* [2000], which is shown in Figure 3c. It is clear that  $T'$  are still too large above 40 km which arises mainly due to ionospheric residuals [*Rocken et al.*, 1997; *Syndergaard*, 2000], hence our studies will be restricted to lower heights. Another practical difficulty using this high pass filter arises near the tropopause especially in the tropics, where a sharp tropopause frequently exists. Therefore the estimation of  $E_p$  using high pass filter is also not possible near the tropopause, especially at low latitudes.

Even though this method serves as best to obtain the global morphology of gravity wave energy, some spectral information on gravity waves (amplitude and phase) will be lost due to the low horizontal resolution (200 to 400 km) and spherical symmetry assumptions in the retrieval of vertical profiles of temperature [*Belloul and Hauchecorne*, 1997; *Lange and Jacobi*, 2002, 2003]. Due to these assumptions, very small scale and large scale gravity waves are filtered out and the  $E_p$  values estimated through these  $T'$  will be low. Nevertheless, due to its global coverage one may obtain an overall features of the gravity wave activity at least qualitatively. The inset picture in 3c,d shows the typical profiles of  $T'$  observed between 20 and 25 km height region on the same day. From this picture it is clear that the amplitude observed by CHAMP is smaller when compared to that obtained by radiosonde, and additionally there is a constant phase shift between the two profiles. Figure 3d shows the Brunt-Väisälä frequency squared,  $N^2$ , observed with CHAMP. From the figure it is clear that  $N^2$  is low in the troposphere and shows a rather abrupt transition near the tropopause, while high values of  $N^2$  are observed in the stratosphere as expected. Some of the  $N^2$  values become negative above 40 km, in this case showing superadiabatic conditions, indicating wave breaking provided the temperature analysis is correct. In general, however, these conditions will occur at higher altitudes and hence these values are thought to be due to the incomplete ionospheric corrections implemented in retrieving the temperature profile from radio occultations. Figure 3e shows the vertical profiles of  $E_p$  observed with radiosonde, lidar and CHAMP/GPS occultations on the same day. At most of the heights,  $E_p$  values estimated from ground-based instruments are showing high. Below 10 km there is an unusual increase in the  $E_p$  values, which is mainly due to water vapour effects ignored in retrieving temperature from radio occultations.

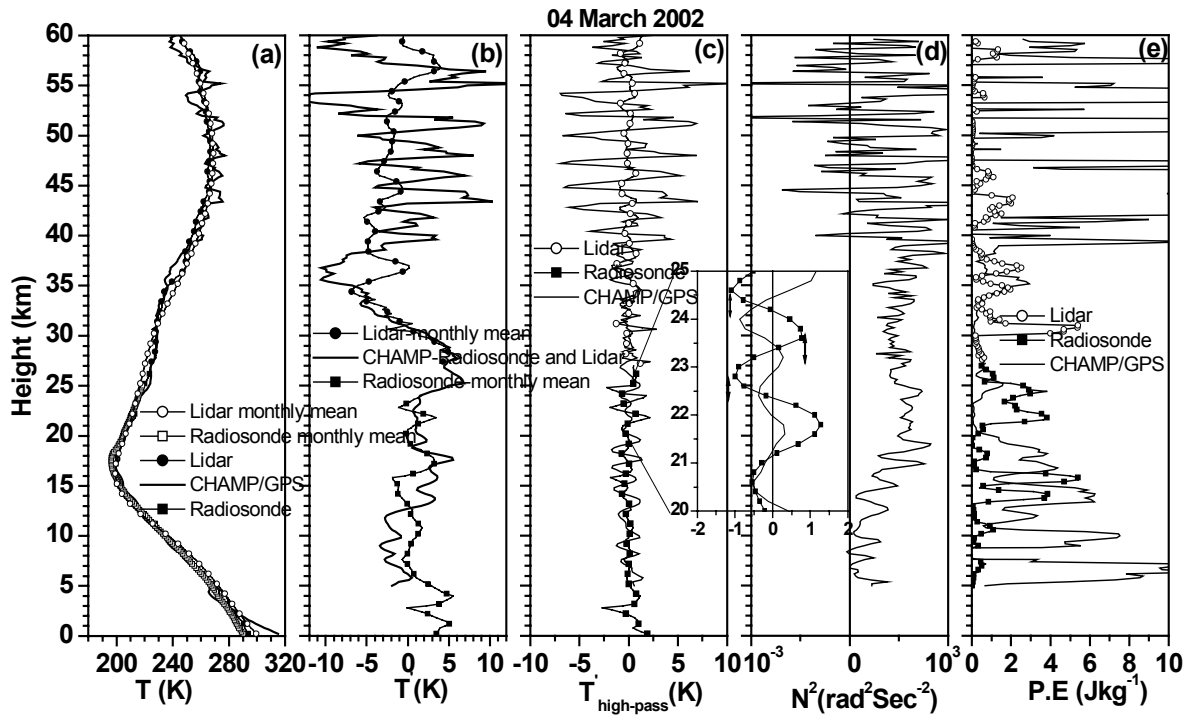


**Figure 3:** Vertical profiles of (a) temperature, (b) temperature perturbation estimated from monthly mean, (c) temperature perturbation estimated from the high pass filter, (d) Brunt-Väisälä frequency square and (e) potential energy observed on March 4, 2002. The inset picture in (c) and (d) shows the practical difficulty in getting the gravity wave properties with satellite observations.

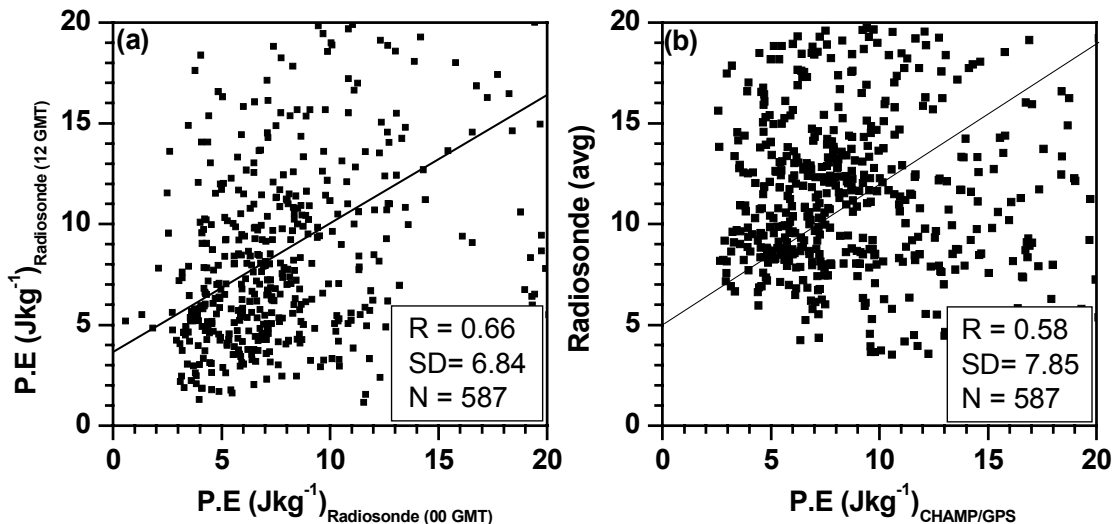


**Figure 4:** Scatter plot of potential energy observed with (a) radiosonde observations at 00 UT and 12 UT, and (b) CHAMP/GPS and radiosonde (average of 00 and 12 UT) observations during June 2001 to May 2002.

Extensive monthly comparison  $E_p$  values observed within the radiosonde observations between 00 UT and 12 UT and also with CHAMP/GPS radio occultations observed during June 2001 to May 2002 are shown in Figure 4. In this figure, only the observed  $E_p$  values between 15 and 25 km are considered. From Figure 4a it is visible that the  $E_p$  values observed at 12 UT are larger than those observed at 00 UT, which might be due to increased daytime gravity wave activity due to convection. It is generally believed that in the tropics and sub tropics, most of the gravity waves are generated by convection [Alexander and Holton, 1997] and strong wind shear [Beres *et al.*, 2002] caused by tropical easterly jet streams. Only for about 66 % of the time,  $E_p$  values observed at both times are similar, and rest of the time the 12 UT values are observed to be larger.. This suggests that there is a need to consider the diurnal variation of  $E_p$  values instead of averaging all the occultations, while presenting global distribution of  $E_p$  using satellite observations. However, since the data base used for the present study consists of only one and half year and it is therefore difficult to obtain global coverage at various times of the day, all available occultations are averaged here while presenting the global morphology of gravity wave activity, leaving the task of analysing the diurnal variation to a further study.

Comparison of  $E_p$  values estimated with radiosonde and CHAMP/GPS in between 15 and 25 km shown in Figure 4b reveals that the radiosonde observed  $E_p$  values are almost 30% larger than those observed with CHAMP/GPS data. This can be attributed to the smaller magnitudes of  $T'$  using the high pass filter of the radio occultation processes. From theoretical estimations, Tsuda *et al.* [2000] found that there will be a up to 21% decrease in the amplitudes of GPS/MET radio occultations. Using a 2D model, Lange and Jacobi [2002] studied the influence of geometric wave parameters and the measurement geometry on plane gravity waves in the range of 100-1000 km horizontal and 1-10 km vertical wavelengths and found that the radio occultations can resolve more than 90% of the simulated gravity waves with 60% amplitude level and more than the 50% of the derived amplitudes are above 90%.

#### 4.3. Global distribution of gravity wave activity in lower stratosphere

The global distribution of  $E_p$  values, observed during the months of December 2001 and March 2002, averaged between 20 and 25 km are shown in Figure 5. The number of occultations used for this figure amounts to 2,921 in December 2001 and 4,149 in March 2002. The number of occultations has been significantly improved after February 2002 onwards. From Figure 5 it is evident that at tropical and subtropical latitudes ( $\pm 30^\circ$  latitude) large  $E_p$  values are noticed in both months, which could be due to large convection expected at those latitudes, and partly may also be due to equatorial waves. Another interesting feature to be noticed in December 2001 is that large values are visible even at mid latitudes on continents, while smaller values are found over the oceans, which is also reported by Tsuda *et al.*, [2000] during northern hemisphere winter months.

However, this feature is not clearly observed during March 2002, which reveals that the large  $E_p$  values observed over the continents are either not modulated due to mountain/lee waves (topography), or modulated but could not propagate to the lower stratosphere. From these two examples it is clear that the gravity wave activity observed with radio occultations will not depend on source distribution at least at stratospheric heights. Perhaps the distribution mainly depends on interactions of propagating gravity waves with the background wind as reported by Alexander, [1998]. It also well known that gravity wave activity will be stronger at mid latitudes in winter [Allen and Vincent, 1995] and at tropical latitudes during equinoxes as observed here.



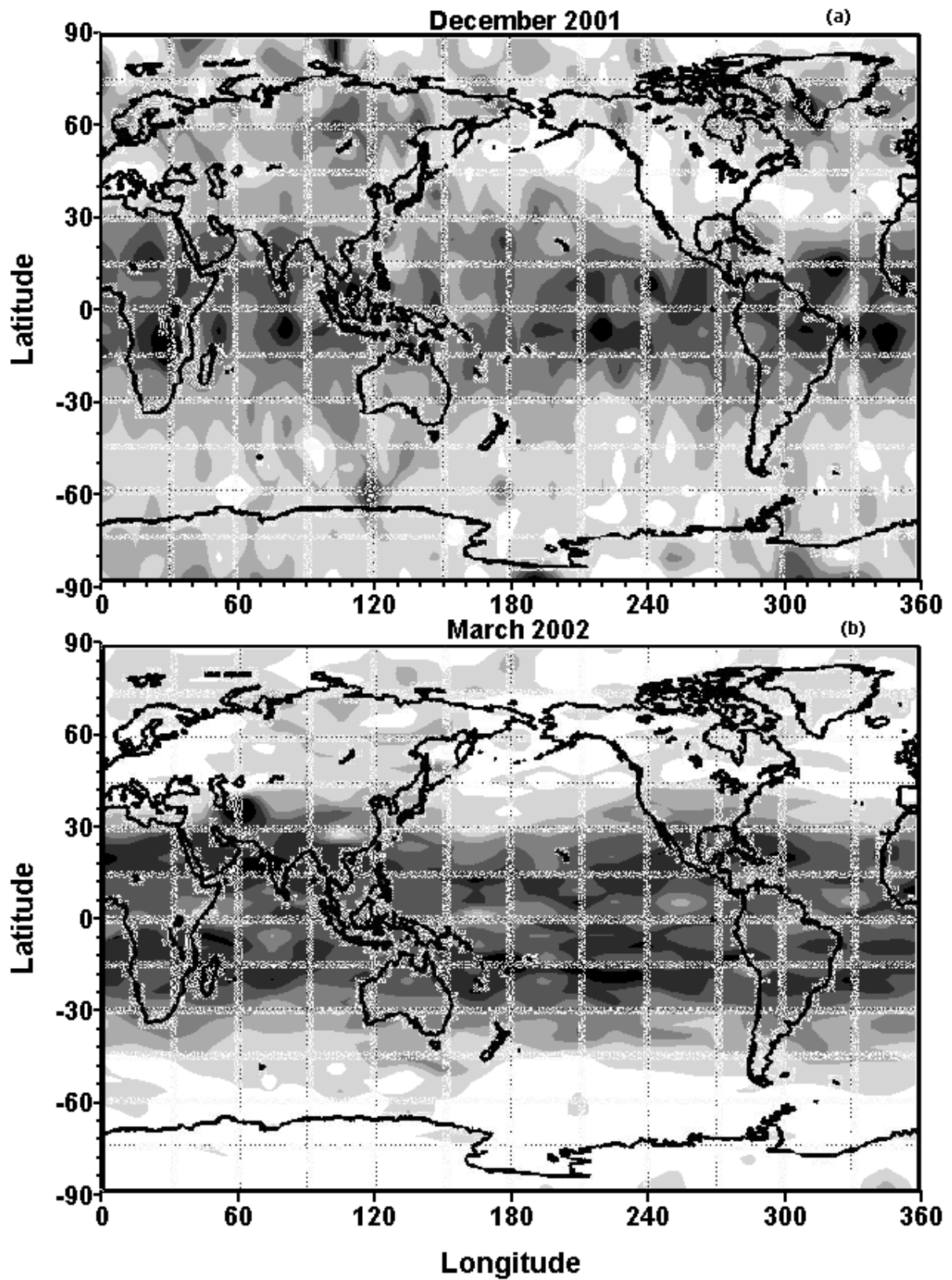


**Figure 5:** Global distribution of gravity wave activity observed in lower stratosphere (20-25 km) during (a) December 2001 and (b) March 2002.  $E_p$  contour intervals are shifted for every 2 J/kg.

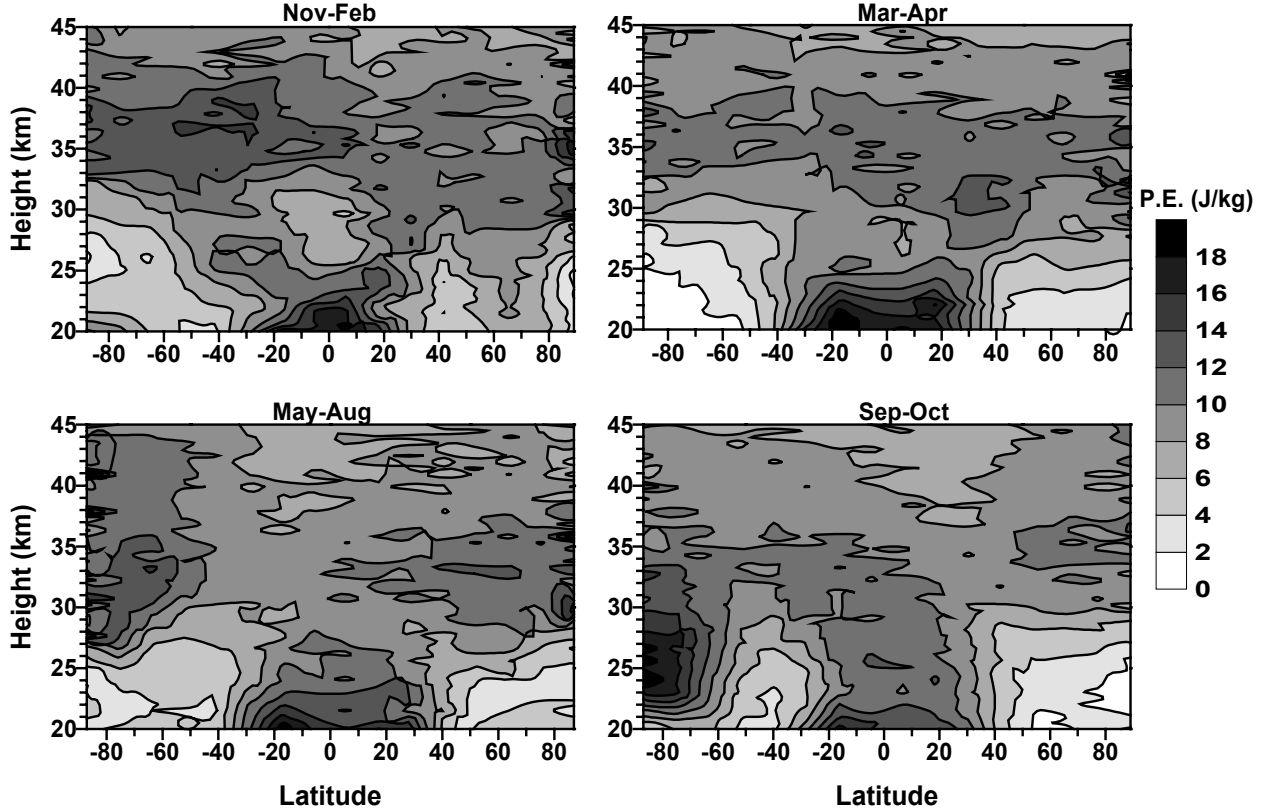


**Figure 6:** Latitudinal variation of potential energy observed in the stratosphere in different seasons during May 2001 through September 2002.

#### 4.4. Latitudinal variation of gravity wave activity

In this section we present the latitudinal variation of  $E_p$  observed during different seasons. NH winter (Nov-Feb), spring equinox (Mar-Apr), summer (May-Aug) and autumn equinox (Sep-Oct). The latitudinal and seasonal variations of  $E_p$  values observed with CHAMP/GPS during May 2001 to September 2002 is shown in Figure 6. The total number of occultations used for this figure are 10,935, 17,429, 8,811 and 7,323 for NH winter, summer, spring and autumn, respectively. The data base used for the present study is almost twice as large as the one used by Tsuda *et al.* [2000], which gives more statistically significant results. Due to improved GPS receiver performance, the amount of profiles reaching the earth's surface is significantly larger than with GPS/MET.

From the Figure 6, salient features noticed are large values of  $E_p$  at low latitudes below 25 km in almost all the seasons. The latitudinal range is wider (up to  $\pm 30^\circ$  at both hemispheres) in all the seasons except winter. During SH winter (May-Aug), large values of  $E_p$  are noticed there. These values are nearly the same at middle latitudes during equinoxes between NH and SH. These values seem to be low between 25 and 30 km near equator especially during winter and summer seasons. At higher latitudes in both hemispheres,  $E_p$  values are larger. During NH spring equinoxes, the latitudinal distribution of  $E_p$  values are nearly symmetric between NH and SH in the entire height ranges. During winter and summer seasons, the  $E_p$  distribution involves a large hemispheric asymmetry at middle and high latitudes, which is more pronounced in NH summer. The  $E_p$  values between  $40^\circ$  and  $60^\circ$ S in Nov-Feb are significantly larger than those at  $40^\circ$  and  $60^\circ$ N. Similarly,  $E_p$  values in between  $40^\circ$  and  $70^\circ$ S in Nov-Feb are significantly larger than those observed in between  $40^\circ$  and  $80^\circ$ N in May-Aug. Another interesting feature noticed is that large values of  $E_p$  are found at SH polar latitudes

during Sep-Oct. Most of the features mentioned above are also noticed by *Tsuda et al.*, [2000] using GPS/MET radio occultations. The only difference noticed is still the wider latitudinal range of large equatorial values and the large values of  $E_p$  at SH polar latitudes during Sep-Oct. Investigations are still going to know the possible reason for this significant enhancement and wider latitudinal range.

## 5. Summary and conclusions

Preliminary observations on a global analysis of gravity wave activity in the stratosphere is presented. The analysis is based on perturbations observed in the vertical temperature profiles of GPS radio occultation onboard CHAMP. Initially, vertical profiles of temperature (10-45 km) observed with CHAMP/GPS are compared with ground based instruments, namely radiosonde (between 10 and 30 km) and Lidar (30-45 km). In general, good agreement is found between these different techniques. The potential energy is calculated from the perturbations of the temperature (2 to 10 km) and the background Brunt-Väisälä frequency. Monthly  $E_p$  values are calculated with radiosonde observations and are compared with those estimated with CHAMP/GPS in order to estimate the accuracy of the satellite measurements. In general,  $E_p$  values estimated with radiosonde observations are found to be larger than those estimated with radio occultations, which may be due to horizontal resolution and spherical symmetry assumptions implemented in the retrieval of the temperature profiles from radio occultations.

Making use of the advantage of high accuracy and vertical resolution along with global coverage of CHAMP/GPS satellite observations, global and seasonal variations of  $E_p$  are studied. From monthly variations it is found that the gravity wave activity is larger at mid latitudes during winter and also larger at tropical latitudes during equinoxes. Global and seasonal variations reveal that the largest values of  $E_p$  are noticed at low latitudes below 25 km in all seasons. During SH winter, largest values of  $E_p$  are noticed, while during equinoxes,  $E_p$  values at mid latitudes are nearly the same in both hemispheres.  $E_p$  values are found to be very low between 25 and 30 km near the equator especially during solstice. It is also found that there is a large hemispheric difference in  $E_p$  values during solstice conditions. An interesting feature noticed is that large values of  $E_p$  at SH polar latitudes during autumn equinox occur, and strong temporal variations of stratospheric gravity wave activity are found.

The investigations cannot be considered as finished, however, for two reasons. Here we used level 2 GPS data from GFZ Potsdam, while very recently a new version has become available. It is expected that further improvements especially at higher altitudes will lead to a more detailed  $E_p$  analysis there. In addition, the data base used should be increased to obtain a higher statistical significance of the monthly mean results. This should enable us to derive reliable monthly climatologies of the stratospheric gravity wave activity, which may be used in numerical circulation models to obtain a more realistic gravity wave parameterisation.

## Acknowledgements

We wish to thank GFZ Potsdam for providing CHAMP/GPS data through the ISDC data centre. This research was funded by the DFG under grant JA 836/4-2.

## References

- Alexander, M. J., Interpretations of observed climatological pattern in stratospheric gravity wave variance, *J. Geophys. Res.*, **103**, 8627-8640, 1998.
- Alexander, M. J., and J. Holton, A model study of zonal forcing in the equatorial stratosphere by convectively induced gravity waves, *J. Atmos. Sci.*, **54**, 408-419, 1997.

- Alexander, M. J., J. H. Beres, and L. Pfister, Tropical stratospheric gravity wave activity and relationship to clouds, *J. Geophys. Res.*, **105**, 22,299-22,309, 2000.
- Allen, S. J., and R. A. Vincent, Gravity wave activity in lower atmosphere: Seasonal and latitudinal variations, *J. Geophys. Res.*, **100**, 1327-1350, 1995.
- Belloul, M. B., and A. Hauchecorne, Effect of periodic horizontal gradients on the retrieval of atmospheric profiles from occultation measurements, *Radio Sci.*, **32**, 469-478, 1997.
- Beres, J. H., M. J. Alexander, J. R. Holton, Effects of tropospheric wind shear on the spectrum of convectively generated gravity waves, *J. Atmos. Sci.*, **59**, 1805-1824, 2002.
- Fritts D.C. and T.E. VanZandt, Effects of Doppler Shifting on the Frequency Spectra of Atmospheric Gravity Waves, *J. Geophys. Res.*, **92**, 9723-9732, 1987.
- Fritts, D. C and Nastrom, G. D., Sources of mesoscale variability of gravity waves II: frontal, convective and jet stream excitation, *J. Atmos. Sci.*, **49**, 111-127, 1992.
- Garret, C., and W. Munk, Space-time scales of internal waves, *Geophys. Fluid Dyn.*, **3**, 225-264, 1972.
- Garrent, C., and W. Munk, Space-time scales of internal waves: A progress report, *J. Geophys. Res.*, **80**, 291-297, 1975.
- Hocke, K., Inversion of GPS meteorology data, *Ann. Geophys.*, **15**, 443-450, 1997.
- Kiffaber LM, Friesen DR, Knutson DL and Peterson AW, Short gravity wave periodicities during AIDA, *J. Atmos. Terr. Phys.*, **55**, 341-354, 1993.
- Lange, M., and Ch. Jacobi, Analysis of gravity waves from radio occultation measurements, *Meteorologische Arbeiten aus Leipzig VII*, **26**, 101-108, 2002.
- Lange, M., and Ch. Jacobi, Analysis of gravity waves from radio occultation measurements, *Proceedings of the First CHAMP Science Meeting*, 22.-25.1.2002, Potsdam, Springer Series, in press, 2003.
- McLandress, C., M. J. Alexander, and D. L. Wu, Microwave limb sounder observations of gravity waves in the stratosphere: A climatology and interpretation, *J. Geophys. Res.*, **105**, 11,947-11,967, 2000.
- Nastrom, G. D., A. R. Hansen, T. Tsuda, M. Nishida, and R. Ware, A comparison of gravity wave energy observed by VHF radar and GPS/MET over central North America, *J. Geophys. Res.*, **105**, 4685-4687, 2000.
- Piani, C., D. Durran, M. J. Alexander, and J. R. Holton, A numerical study of three-dimensional gravity waves triggered by deep tropical convection and their role in the dynamics of the QBO, *J. Atmos. Sci.*, **57**, 3689-3702, 2000.
- Reigber, C., H. Lühr, and P. Schwintzer, CHAMP mission status and perspectives, *Suppl. to EOS*, Transactions, AGU, **81**, 48, F307, 2000.
- Rocken, C., R. Anthes, M. Exner, D. Hunt, S. Sokolovskiy, R. Ware, M. Gorbunov, W. Schreiner, D. Feng, B. Herman, Y.-H. Kuo, X. Zou, Analysis and validation of GPS/MET data in the neutral atmosphere, *J. Geophys. Res.*, **102**, 29849-29866, 1997.
- Scheffler A.O. and C.H. Liu, On observation of gravity wave spectra in the atmosphere by using MST radars, *Radio Sci.*, **20**, 1309-1322, 1985.
- Scheffler, A.O., and C.H. Liu, The effects of Doppler shift on gravity wave spectra observed by MST radar, *J. Atmos. Terr. Phys.*, **48**, 1225-1231, 1986.

- Syndergaard, S., On the ionosphere calibration in GPS radio occultation measurements, *Radio Sci.*, **35**, 865-883, 2000.
- Tsuda, T., M. Nishida, C. Rocken, and R. H. Ware, A global morphology of gravity wave activity in the stratosphere revealed by the GPS occultation data (GPS/MET), *J. Geophys. Res.*, **105**, 7257-7273, 2000.
- VanZandt, T.E., A universal spectrum of buoyancy waves in the atmosphere, *Geophys. Res. Lett.*, **9**, 575-578, 1982.
- VanZandt, T.E., A model for gravity wave spectra observed by Doppler sounding systems, *Radio Sci.*, **20**, 1323-1330, 1985.
- Wickert, J., C. Reigber, G. Beyerle, R. König, C. Marquardt, T. Schmidt, L. Grunwaldt, R. Galas, T. K. Meehan, W. G. Melbourne, and K. Hocke, Atmospheric soundings by GPS radio occultation: First results from CHAMP, *Geophys. Res. Lett.*, **28**, 3263–3266, 2001.
- Wu, D. L., and J. W. Waters, Satellite observations of atmospheric variances: A possible indication of gravity waves, *Geophys. Res. Lett.*, **23**, 2631-2634, 1996.

#### **Addresses of Authors**

Christoph Jacobi, M. Venkat Ratnam, Institut für Meteorologie, Universität Leipzig, Stephanstr. 3, 04103 Leipzig, jacobi@uni-leipzig.de, vratnam@uni-leipzig.de